Organic Process Research & Development

Article

pubs.acs.org/OPRD

A Flow-Based Synthesis of 2-Aminoadamantane-2-carboxylic Acid

Claudio Battilocchio,*[,†,‡] Ian R. Baxendale,[†] Mariangela Biava,[‡] Matthew O. Kitching,[†] and Steven V. Ley[†]

[†]Department of Chemistry, University of Cambridge, Lensfield Road, Cambridge CB2 1EW, United Kingdom

[‡]Dipartimento di Chimica e Tecnologie del Farmaco, "Sapienza" Università di Roma, P.le A. Moro 5, Roma 00185, Italy

Supporting Information

ABSTRACT: The development of a new, high-yielding, scalable and safe process for the preparation of 2-aminoadamantane-2-carboxylic acid (**1**) is described. This geminal, functionalized achiral amino acid has been reported to possess interesting biological activity as a transport mediator due to its unique physiochemical properties. We report herein on the use of various mesoreactor flow devices to expedite the lab-scale synthesis of this molecule by simplifying the processing requirements for use of several potentially hazardous reagent combinations and reaction conditions.

INTRODUCTION

The adamantyl cage is an important motif[1] present in numerous biologically active compounds including a number of currently used therapeutic agents (Figure 1).[2] The unique symmetrical yet configurationally rigid geometry of the adamantane cage is often used to influence a structure's physiological properties by providing a bulky lipophilic scaffold.[3] One particularly interesting adamantane derivative, namely, 2-aminoadamantane-2-carboxylic acid (**1**), is an unnatural, achiral amino acid which has been shown to possess novel transport inhibitory properties (Figure 2).[4] According to Tager and Christensen,[5] this molecule perfectly fulfills the theoretical requirements for transport inhibition of amino acids: (a) bulky side chain, (b) side chain apolarity, (c) catabolic resistance for the presence of a tertiary α-carbon, and (d) sufficient water solubility. We became interested in the synthesis of this amino acid as part of a research program directed towards the preparation of key probes for neurotensin receptors 1 and 2 (NTR1 and NTR2).[6a] NTR1 and 2 are both seven-transmembrane G protein-coupled receptors (GPCR's) with increasing relevance in several human cancers.[6] In the early 1990s, Sanofi-Aventis in a high throughput screening campaign identified SR 45398 (**2**)[7] as a binder of NTR in guinea pig brains (IC_{50} 40 μm). Through iterative lead optimization, this was developed into the NTR1 antagonist Merclinertant SR 48692 (**3**)[7,8] and then a second-generation analogue SR 142948A (**4**)[9] capable of preferentially activating NTR 2. In these molecules, the 2-aminoadamantane-2-carboxylic acid residue, **1**, is reported to be responsible for key interactions allowing the selective recognition of the NTR receptor.[10]

Wishing to prepare large quantities of both SR 48692 (**3**) and SR 142948A (**4**), we required a scalable and reliable route to this key fragment.

DISCUSSION

Evaluating the preparative routes currently reported in the literature we identified two main synthetic strategies. Our initial investigations employed a Bucherer–Berg reaction as described by Nagasawa (Scheme 1, footnote *a*).[11] In the original report, treatment of ketone **5** with a buffered solution of sodium cyanide at elevated temperature and pressure yielded the spirohydantoin **6** which, without purification, was hydrolysed to the desired amino acid **1** in good overall reported yield.

In order to more readily achieve the necessary elevated reaction temperature and pressure windows as outlined (Scheme 1, footnote *a*) we transposed the chemistry to a Biotage microwave reactor initially using sealed 20 mL reaction vials with only minor modifications of the previous batch route (Scheme 1, footnote *b*). This allowed us to perform the chemistry safely, yielding material identical to that obtained following the original batch conditions. (Note: this is an important point of consideration relating to later discussion concerning product purity.)

Although batch processing of such relatively small volumes was straightforward when conducting optimization and test reactions, a microwave approach can be severely limiting when considering scale-up. It is not possible to directly scale a microwave cavity in order to increase output equivalent to a standard batch reactor. Physical restrictions, pertaining to the defined penetration depth of microwaves into a reactor, limit such an approach or certainly make reactor scaling a major engineering challenge.[12] We circumvented this issue in part by employing a CEM stop-flow microwave.[13] The adoption of stop-flow microwave handling allowed the rapid scale-up of the reaction sequence even though it required the processing of heterogeneous slurries (hydantoin input reaction solution and the resulting product mixture). Furthermore, the continuous monitoring of temperature and pressure combined with automatic safety cutoffs also minimized the risks associated with scale-up. Of particular value was the automation of the entire process which ensured reproducibility across the consecutively conducted batch operations whilst lowering the manual handling time necessary for a skilled chemist. In this fashion, material could be quickly processed through the two-step sequence on >400 mmol scale.

Unfortunately, in our hands, isolation of the pure amino acid **1** was not possible. Following either the original reported

Received: March 27, 2012
Published: April 17, 2012

 © 2012 American Chemical Society dx.doi.org/10.1021/op300084z | *Org. Process Res. Dev.* 2012, 16, 798–810

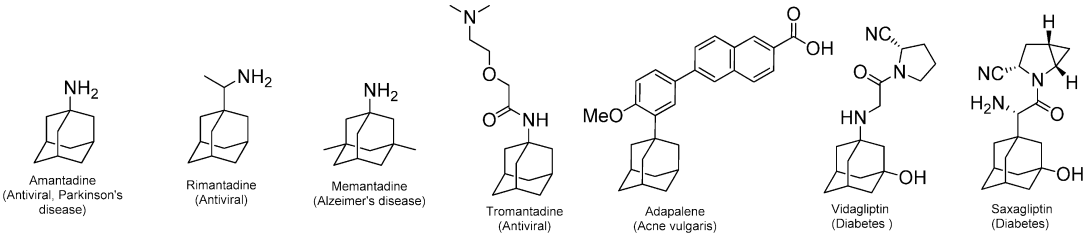

Figure 1. Adamantyl-containing therapeutics in current clinical use.

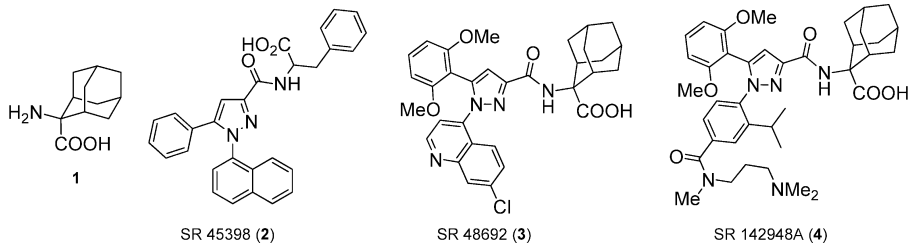

Figure 2. 2-Aminoadamantane-2-carboxylic acid (**1**) and Sanofi-Aventis' SR 45398 (**2**), Merclinertant SR 48692 (**3**) and SR 142948A (**4**).

Scheme 1. Nagasawa's route to the amino acid 1;[a] microwave processing conditions[b]

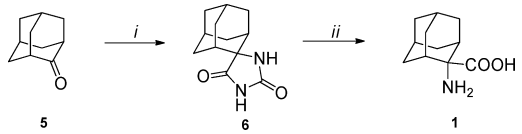

[a]Reaction conditions: i) NaCN (2 equiv), $(NH_4)_2CO_3$ (1.5 equiv), EtOH, 120 °C, 170 psi, 3 h (99%); ii) 1.25 N NaOH, 195 °C, 250 psi, 2 h (81%). [b]Reaction conditions: i) NaCN (2.2 equiv), $(NH_4)_2CO_3$ (1.5 equiv), EtOH/H_2O (3:1), 150 °C, 2 h (94%); ii) 1.25 N NaOH, 175 °C, 3 h (71%).

procedure[11] or our modified microwave protocol gave material that was always significantly contaminated by unidentifiable inorganic impurities as determined by microanalysis (compound **1**, observed range C = 37−45%, desired 67.7%).[14] It also proved extremely difficult to purify this final amino acid product **1** due to its limited solubility. We therefore decided to break the route down into its component steps and investigate the individual processes in more depth.

First, confirmation of the extent of the hydantoin hydrolysis step and determination of the level of inorganic impurities at this intermediate stage were assessed by ^{1}H NMR analysis (in D_2SO_4). In order to facilitate rapid calibration and allow quantification of the levels of components, each analytical sample was doped with known quantities of *p*-anisidine to act as an internal standard. From this investigation it was evident that hydantoin **6** was being successfully and fully hydrolysed to the corresponding amino acid **1** under the prescribed reaction conditions. However, it was also clear that the synthesized hydantoin material **6** possessed on average only 30−35% of the desired material by mass. All attempts to enhance the quality of this intermediate material by hot filtration through Celite or glass wool, or by treatment with charcoal, Fuller's Earth, or montmorillonite clays surprisingly failed to significantly improve its quality (≤45% purity by mass). Furthermore, recrystallisation from various solvent systems proved only moderately effective, leading to very poor recovery and only partially purified intermediate **6** (≤80% purity). Eventually analytically pure material was realized through repeated recrystallisation from THF (four cycles) to yield the desired hydantoin **6** as its monohydrate complex.

Subjecting the purified hydantoin **6** independently to the subsequent hydrolysis step showed that this transformation occurred in a manner identical to that of the reactions of the crude material. As monitored by ^{1}H NMR of the reaction mixture (in D_2SO_4), complete conversion to the amino acid **1** could be achieved by utilizing microwave heating under basic conditions; however, frustratingly problems still persisted regarding isolation of the amino acid. All attempts to maximize the recovery of the product yielded material of much lower purity (best result being 72% isolated yield corresponding to an elemental analysis indicating only 80% purity). We were therefore forced to consider alternative synthesis procedures.

As initially stated, a second synthetic strategy was also originally identified in the literature. We therefore turned our attention to this alternative pathway as inspired by Commeyras[15a−c] and Edward[15d] which utilized a key Strecker reaction (Scheme 2). Commeyras had identified a mild method of

Scheme 2. Edward route to the amino acid 1

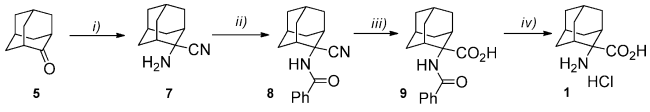

catalyzing the hydrolysis of nitriles (Strecker adducts) via an in situ generated aminol intermediate (Figure 3). Edward built upon this concept using the presence of an α-amido moiety to facilitate an intramolecular attack upon the adjacent nitrile, forming the more reactive cyclic intermediate **11** which in turn was rapidly hydrolysed to the corresponding α-aminoamide **12** and then more slowly to acid **9** (Figure 4).

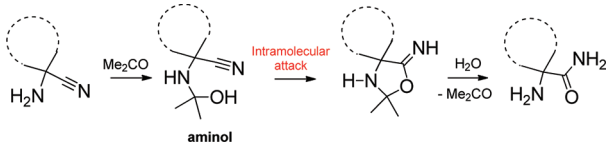

Figure 3. Commeyras-assisted hydrolysis of α-amino nitriles.

dx.doi.org/10.1021/op300084z | Org. Process Res. Dev. 2012, 16, 798−810

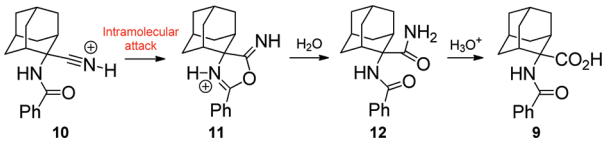

Figure 4. Edward-assisted hydrolysis to give amino acid **9**.

Following a minor modification of the Edward route we obtained the required amino acid **1** in essentially comparable overall yield (Scheme 2). The isolated product was also deemed to be free from inorganic impurities as determined by microanalysis. An additional benefit of this process was also realized with regards to the ease of monitoring the final reaction steps, owing to the presence of a UV chromaphore (the benzamide group). Despite these apparent advantages, attempts to scale up the process led to a marked decrease in the reaction yields and an equivalent drop in the purity of the intermediates, especially for the transformations of **7** and **9** which decreased noticeably to 48% and 56%, respectively, on a 50 mmol scale (73% and 89% previously).

We therefore decided to investigate a completely new approach to **1** which would also be amenable to continuous scale-up through the adoption of flow reactor technologies.[16] Although the proposed route was based on a slightly longer five-step sequence, we envisaged that each of the iterative steps would be both individually high yielding and readily scaled under flow conditions (Figure 5). The sequence would commence with a Grignard reagent addition to 2-adamantanone (**5**) followed by conversion of propargylic alcohol **13** to the acyl-propargylamide derivative **14** via a Ritter reaction. A subsequent 5-enol-*exo-dig* cyclisation would furnish the oxazole intermediate **15** on route to the azalactone **16** via ozonolysis. This heterocyclic material **16** would represent a valuable precursor in that it could be readily hydrolyzed to the desired amino acid **1** but as its self possess inherent reactivity as a masked carboxylic acid coupling partner.[17]

Synthetic Step 1: Grignard Addition. Initially it was envisioned that this reaction would need to be performed at subzero temperatures due to the well-precedented reversibility of the Favorskii reaction under basic conditions.[18] Indeed, under batch conditions, if the propargyl alcohol anion was allowed to warm to temperatures above −10 °C prior to quenching, substantial quantities of the starting ketone were isolated.

We therefore conducted the Grignard addition at −20 °C, employing a cryo-flow reactor[19] equipped with a 52 mL perfluoroalkoxy polymer (PFA) reactor coil and two 1 mL PFA precooling loops. A 0.5 M solution of 2-adamantanone (**5**) in THF and a 0.5 M THF solution of ethynylmagnesium bromide were delivered at a flow rate of 0.2 mL min^{-1} to the precooling loops and then combined thereafter in the reactor coil via a T-connector. Using this setup we were able to obtain an approximate 50% yield when processing 10 mmol of the substrate. Attempts to optimize the reaction by increasing the residence time or altering the relative stoichiometries of the reagents failed to appreciably change the resulting yield. Eventually we discovered the cryogenic conditions were actually detrimental to the reaction progress in flow. When the reaction was instead carried out at a higher temperature of 40 °C using a 14 mL reactor coil on a Uniqsis FlowSyn system under optimized conditions (0.5 M solution of 2-adamantanone (**5**) in THF at 0.18 mL min^{-1} and 0.5 M solution of ethynylmagnesium bromide in THF at 0.2 mL min^{-1}), we obtained 2-ethynyl-2-adamantanol (**13**) in 80% isolated yield on a 0.30 mol scale after standard aqueous extraction. We prescribe this notable difference in stability of the intermediate to the flow processing regime which means that the ionic concentration of the reaction mixture remains relatively constant throughout the short reaction window. This is different from the corresponding batch scenario where, as the reaction progresses, the concentration and consequently the pH of the reaction media steadily increases, eventually favoring the retro reaction. This is also consistent with observations based upon corresponding batch reactions. It was noted that proportionally higher relative conversion to the desired product was achieved using lower stoichiometries of the Grignard. Also higher final isolated yields were obtained when the reaction was worked up immediately following Grignard addition.

As the potential liberation of acetylene constitutes a worrying safety concern, we were very interested in evaluating the stability of this key intermediate **13**. We therefore conducted a differential scanning calorimetry (DSC) study on this compound (Figure 6). This highlighted an exothermic event which indicated liberation of acetylene being accompanied with a corresponding increase in system pressure at temperatures above 160 °C. To confirm the identity of the suspected degradation product as 2-adamantanone (**5**) we performed a repeat scan on the same sample following cooling. The new data obtained from the recycled sample convincingly matched the profile obtained from authentic 2-adamantanone (**5**); in conclusion, the high-temperature heating caused the de-ethynylation of 2-ethynyladamantan-2-ol (**13**) (Figure 7).[20]

Due to the inherent reversibility of the prop-2-yn-1-olate formation and knowledge that the acidic workup of this anion is exothermic, we considered it to be beneficial to use flow micromixing to prevent any overheating when conducting the quenching step. A straightforward modification of the original setup to incorporate an inline addition of a saturated solution of NH_4Cl was made by the incorporation of a second T-piece (Figure 8). However, this initially proved problematic due to the rapid precipitation of magnesium salts which accumulated over time in the T-connector and eventually resulted in blockage of the reactor. A simple solution to this problem was to use pulsed sonication where the T-piece connector and a short length (10 cm) of the subsequent tubing were submerged in the water bath of a standard laboratory sonicator.[21] This completely eliminated buildup of precipitates, enabling steady-state operation. The product could then be processed

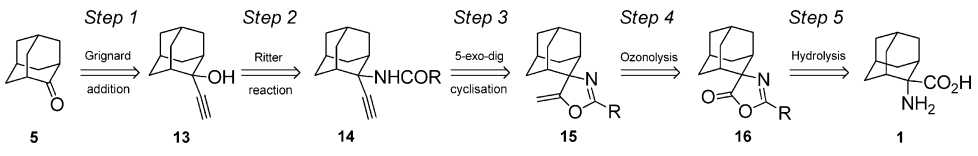

Figure 5. Proposed synthesis to 2-aminoadamantane-2-carboxylic acid (**1**).

dx.doi.org/10.1021/op300084z | *Org. Process Res. Dev.* 2012, 16, 798−810

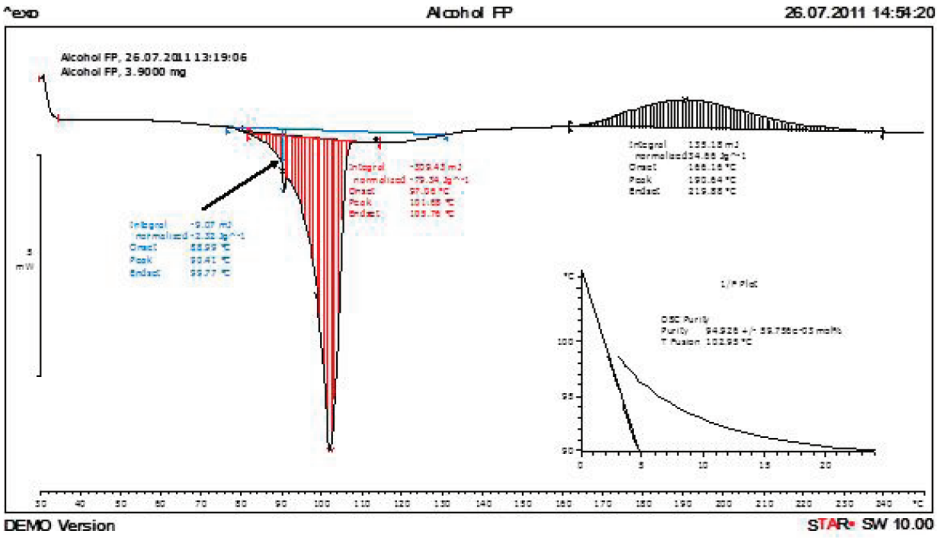

Figure 6. DSC spectrum of the ethynyl derivative: the first "negative" curve is an endothermic melting of the compound; the second "positive" curve is related to its exothermic degradation.

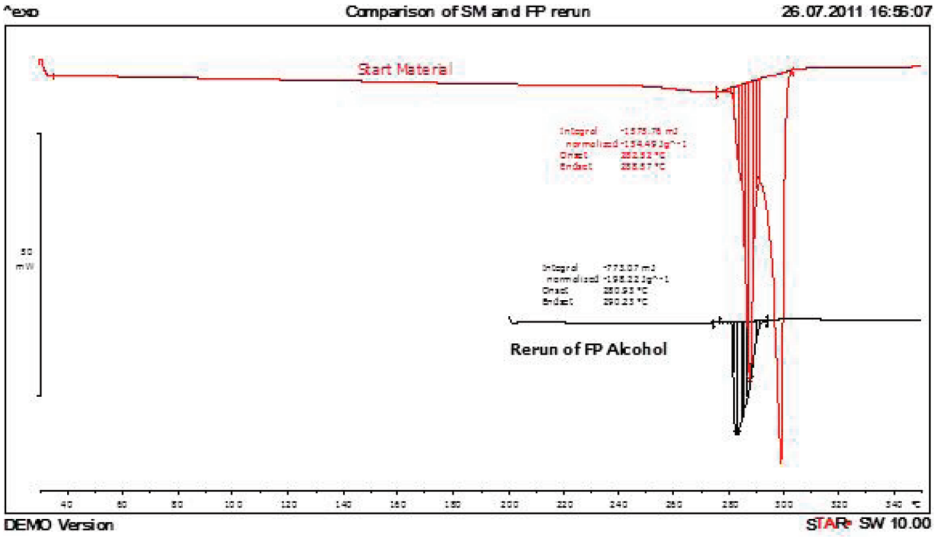

Figure 7. DSC scanning of 2-adamantanone and degradation product of 2-ethynyladamantan-2-ol.

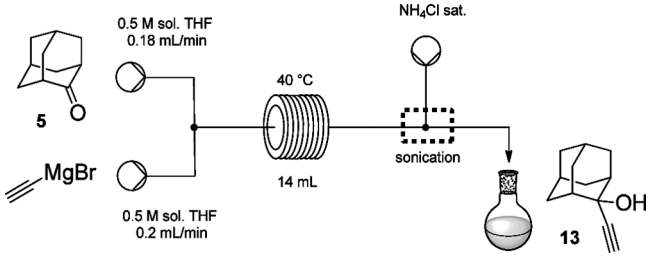

Figure 8. Flow scheme for the optimized Grignard addition with inline quenching.

continuously (longest run 0.66 mol) giving an improved isolated yield of 90%.

Synthetic Step 2: Ritter Reaction. Wirth and co-workers have previously described the feasibility of conducting the Ritter reaction in microfluidic flow devices.[22] They convincingly demonstrated that, even at mild temperatures ranging from 45 to 85 °C depending on the substrate, high conversions could be realized in only a few minutes residence time (~10 min). By combining their results with our own experience gained performing the fluoro Ritter reaction on styrenes[23] we were able to rapidly devise conditions for the adamantane substrate **13**. We selected two different nitriles, namely, benzonitrile and acetonitrile, since these would generate amides with differing electronic natures thereby influencing the subsequent cyclisation and also the potential ease of their eventual deprotection.

The preliminary reaction setup employed two injection loops (3 mL each), one filled with a mixture of the alcohol **13** and the nitrile and the other containing neat concentrated sulfuric acid. These were simultaneously switched into the main flow stream (glacial acetic acid/acetic anhydride, 10:1 [v/v]) combining at a T-piece before progressing into a 14 mL PFA continuous flow coil (CFC). It was quickly determined that temperature was a crucial parameter (principle component analysis, [PCA]); all attempts to perform the reaction at temperatures exceeding 40 °C gave substantial byproduct formation, later identified as arising from a Meyer−Schuster rearrangement followed by a subsequent 1,2-hydride migration (Wagner−Meerwein rearrangement) (Figure 9). At an operating temperature of 30 °C

dx.doi.org/10.1021/op300084z | Org. Process Res. Dev. 2012, 16, 798−810

this product was only present in trace amounts allowing the desired adduct to be isolated in yields of around 85% on a 3 mmol scale.

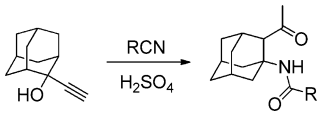

Figure 9. Main product isolated at temperature above 40 °C.

Since the use of large volumes of concentrated sulfuric acid gave workup issues, especially when scaling, we further investigated the performance of the reaction using different solvent compositions and additives. Ultimately, the best results were obtained using a mixture of H_2SO_4/AcOH/Ac_2O, 5:11:5 (v/v/v). Under these optimized conditions, a solution of nitrile/AcOH/**13** was introduced to the system at a flow rate of 1.0 mL min^{-1}. A corresponding solution of H_2SO_4/AcOH/Ac_2O also at a flow rate of 1.0 mL min^{-1} was directed to meet the first stream at a mixing-T piece prior to entering a 14 mL PFA CFC maintained at 30 °C (Figure 10). The output stream

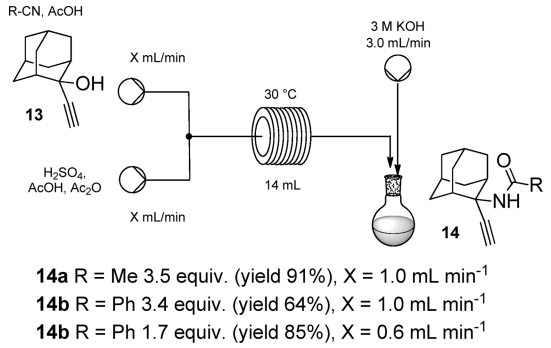

Figure 10. Ritter flow scheme for the synthesis of propargylamide **14**.

was collected into a continuously stirred tank reactor which was continuously quenched and neutralized by an auxiliary feed line delivering a solution of aqueous KOH (3 M). Periodically the flask was exchanged and the solution extracted with DCM, allowing isolation of the Ritter product **14** (Figure 10). The lower yield obtained in the case of amide **14b** is a consequence of its problematic separation. Indeed, determination of the crude conversion to benzamide **14b** indicated >95% by ^{1}H NMR and LC−MS. However, upon scale-up the excess benzonitrile and its resulting hydrolysis byproduct (benzamide) created considerable issues regarding efficient and clean extraction of the product from the reaction media. Some success was eventually realized by reducing the excess of benzonitrile (to 1.7 equiv), and increasing the residence time, thereby allowing isolation of an improved 85% of the amide product **14b**. Unfortunately, isolation still remained a significant issue at larger scales (i.e., >25 g) with no satisfactory alternative workup conditions being readily identified (see later discussion for a solution).

Synthetic Step 3: 5-Enol-*exo-dig* Cyclisation. In order to rapidly scope out the potential options for the formal 5-enol-*exo-dig* cyclisation we evaluated a series of parallel batch conditions. Attempts to catalyze the cyclisation of the propargylamides **14** with various metal salts such as silver, copper, or gold were only partially successful.[24] The best results were obtained using silver hexafluoroantimonate (DCM, rt) leading to 65% conversion although we were discouraged from its use at scale due to cost. Interestingly, the use of sodium hydroxide in a biphasic toluene/water mixture in the presence of tetrabutylammonium chloride as a phase transfer catalyst allowed isolation of the product **15** in a 50% yield.

Further profiling of the reaction by screening various bases, concentrations, temperatures, and reaction times highlighted a combination of potassium hydroxide in ethanol as an improved media. Therefore, when a ∼3:1 molar ratio of KOH to starting material **14** in EtOH (1.3 M) was microwave irradiated at 100 °C for 2 h, a high isolated yield of the desired product was obtained (around 90%). At higher temperatures the reactions produced larger quantities of an unidentified byproduct (Figure 11). Interestingly, the tailored conditions for the corresponding

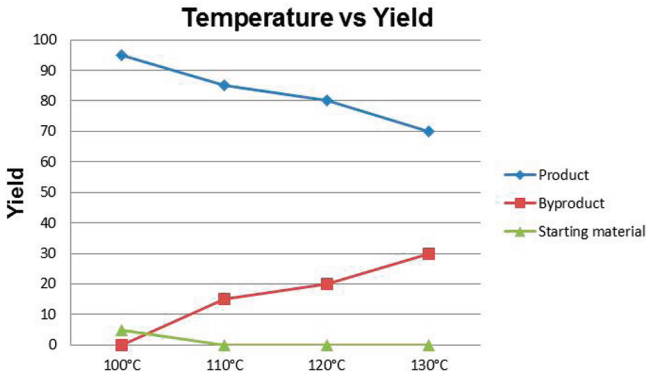

Figure 11. Temperature-dependent 5-enol-*exo-dig* cyclisation of **14a**.

flow procedure allowed the use of an elevated temperature window with a correspondingly shorter reaction time without the accompanied byproduct formation (Table 1 and 2).

Table 1. Flow optimization of the acetamide derivative cyclisation 15a

entry	residence time (min)	temperature °C	conversion % (isolated yield %)
1	24	100	57 (57)
2	48	100	74 (74)
3	7	120	53 (53)
4	24	120	80 (78)
5	48	120	100 (91)[a]
6	60	120	100 (85)
7	24	130	100 (60)
8	48	130	100 (45)

[a]No byproduct formation was detected.

In summary, the efficient flow cyclisation of the benzoyl propargylamide derivative **15b** occurred at 120 °C, with a residence time of 24 min (1:16 molar ratio amide **14b** to KOH). The corresponding acetyl derivative **14a** was less reactive, requiring a prolonged residence time (48 min) to achieve complete conversion to the desired product **15a** under the same reaction conditions (Figure 12). In both cases an overall high yield of the cyclised products could be realized, following a very trivial organic extraction of the reactor output.

This facile workup prompted us to consider a telescoped process involving the above cyclisation step in conjugation with the previous Ritter reaction. We anticipated that the basic quenching step used in the Ritter process (Figure 10) could be modified to promote the subsequent cyclisation step (Figure

dx.doi.org/10.1021/op300084z | *Org. Process Res. Dev.* 2012, 16, 798−810

Table 2. Flow optimization of the benzamide derivative cyclisation 15b

entry	residence time (min)	temperature °C	conversion % (isolated yield %)
1	7	100	50 (50)
2	14	100	60 (60)
3	24	100	72 (72)
4	48	100	80 (80)
5	7	120	60 (60)
6	14	120	84 (84)
7	24	120	100 (92)[a]
8	7	130	69 (50)
9	14	130	100 (65)
10	24	130	100 (50)

[a]No byproduct formation was detected.

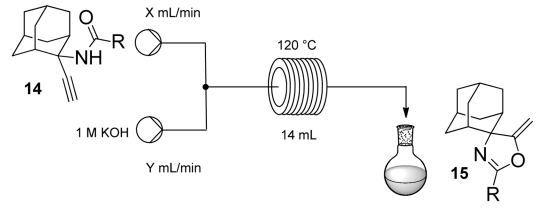

14a → **15a** R = Me (yield 91%), X = 0.2 and Y = 0.1 mL min^{-1}
14b → **15b** R = Ph (yield 92%), X = 0.4 and Y = 0.2 mL min^{-1}

Figure 12. Flow schemes for the 5-enol-*exodig* cyclisation of compounds **14** to oxazolines **15**.

12) as a single integrated flow process. In addition to shortening the sequence and reducing the manual workup it was anticipated that the basic conditions could facilitate easier extraction of the final product. Previously, a major problem in the Ritter step had been encountered due to the issue of extracting and isolating the product from residual nitrile (excess used in the Ritter) and the corresponding partially hydrolysed byproduct amide (acetamide and benzamide). This was particularly difficult when benzonitrile was used at scale. However, under the strongly basic conditions and higher reaction temperature of the cyclisation step complete hydrolysis of the nitrile (and amide) to the carboxylate should occur making extraction of **15** far easier. The flow reactor setup adopted to run this sequence is shown in Figure 13.

Under the telescoped conditions, a solution of nitrile/AcOH/**13** and a corresponding mixture of H_2SO_4/AcOH/Ac_2O were introduced to a 14 mL PFA CFC maintained at 30 °C after mixing at a T-piece. The exiting flow stream was further combined at a second T-connector with a solution of

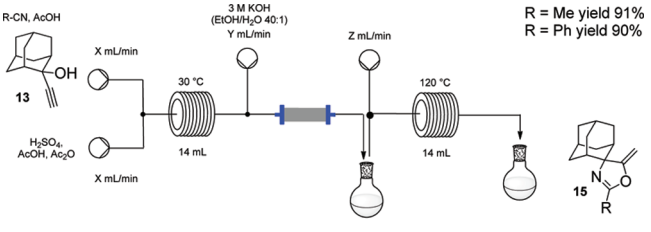

15a R = Me 3.5 equiv. (yield 91%), X = 1.0 mL min^{-1}, Y = 3.0 mL min^{-1}, Z = 0.3 mL min^{-1}
15b R = Ph 1.7 equiv. (yield 90%), X = 0.6 mL min^{-1}, Y = 1.8 mL min^{-1}, Z = 0.6 mL min^{-1}

Figure 13. Combined Ritter reaction and 5-enol-*exodig* cyclisation to oxazolines **15**.

KOH in EtOH/H_2O (3 M, 40:1 [v/v]). Any minor quantities of precipitate were directly removed by inline filtration (glass wool), and the solution was collected into a storage vessel. Following a suitable delay (dependent on the flow rate of the two steps) the eluate was progressed using a second HPLC pump through a heated PFA CFC coil (120 °C). As anticipated, the solution from the reactor could then be readily extracted to give the final product in good yield and excellent purity. This abridged process proved particularly effective for processing larger quantities of material, especially reducing the workup burden.

Synthetic Step 4: Ozonolysis. The oxidative cleavage of the exocyclic alkene was carried out via ozonolysis. Ozone is a well-known oxidizing agent with a broad range of industrial applications spanning chemical synthesis to waste treatment and water purification. Although it has a minimal environmental impact and low cost, it suffers prescriptive use based on safety issues relating to the generation of unstable and highly energetic ozonide intermediates.[25] We and others have already demonstrated the feasibility of conducting flow-based ozonolysis procedures to expedite chemical processing and improve the safety profile of operation.[26] However, many of these systems are not suited to direct scale-up or scale-out parallel application. Consequently, we set ourselves the challenge to develop a simple, high-performance and safe system for the processing of larger quantities of substrate.

The first flow setup (Figure 14) used a Knauer K100 HPLC pump to deliver a sprayed stream of the substrate (0.2 M solution in DCM) into the gas flow (O_2/O_3, 500 mL min^{-1}) via an infusion T-piece (Figure 15b). The combined stream then progressed through a reaction coil (20 mL, 2.5 mm i.d.) with a residence time of 5 min (Figure 15a). The resulting output stream was collected into a vented chamber with the excess ozone being eliminated by gently flushing argon throughout the solution. The expunged solution was then pumped through a packed bed cartridge containing an excess of polymer-supported thiourea,[27] inducing reductive cleavage of the ozonide.[28] The output stream was periodically tested for residual ozone (Ozone Test Kit OZ-2 - Camlabs part no. HH/20644-00) and the presence of unreacted ozonide (via LC−MS by Ph_3P oxidation against an internal standard of 2,3-dimethoxynaphthalene). The output solution was finally evaporated under reduced pressure to give the desired compound **16**.

During the oxidative process we tried to identify the flow pattern in order to help optimize the reaction conditions; the very first portion of the reactor coil (5 cm) was characterized by formation of small liquid droplets along the inner surface of the tubing. This was accompanied by an instantaneous bleaching of the solution (from light yellow to colourless) and a sharp drop in temperature (rt→4 °C as detected by IR measurements at the outer surface of the reactor). We concluded that the endothermic process occurring was related to the "spraying effect" (latent heat of evaporation) that occurred as the liquid phase entered the fast moving gas flow (Figure 15b).[29] Throughout the rest of the coil a wavy/annular flow pattern was observed as shown in Figure 16. Having observed the immediate colour change at the start of the reactor we were interested in determining the composition of the reaction mixture at this stage. Sampling the flow stream after only 18 cm of tubing (1 mL internal volume) indicated total consumption of the starting material which upon treatment with the thiourea resin gave the desired product **16** in quantitative conversion.

dx.doi.org/10.1021/op300084z | Org. Process Res. Dev. 2012, 16, 798−810

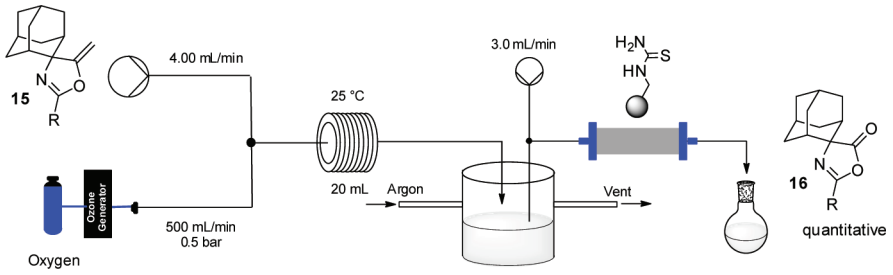

Figure 14. Initial setup for ozonolysis in flow.

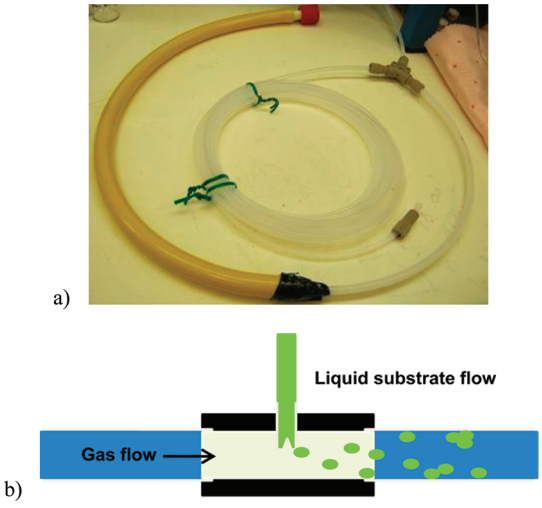

Figure 15. (a) PTFE reactor-coil for ozonolysis in flow. (b) Schematic of T-connector.

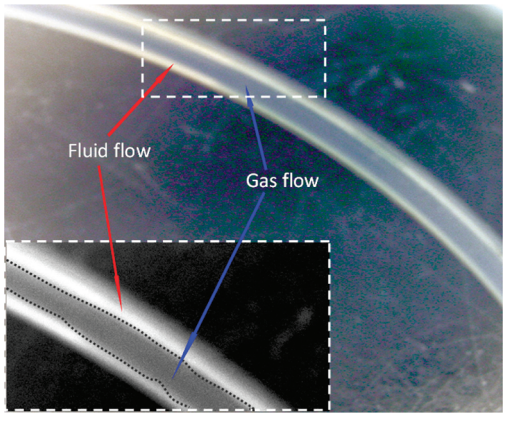

Figure 16. Wavy-annular flow pattern observed inside the PTFE reactor coil in the ozonolysis reaction.

Therefore, wishing to take advantage of this "spraying" phenomenon we envisaged the assembly of a short-path reactor unit with a residence time of only 15 s. In addition to facilitating rapid reaction processing and self-controlled cooling the spray dispersion phenomenon would also assist flushing excess ozone from the reaction stream by showering the output feed into an argon (or nitrogen) blanketed purge vessel (Figure 17). At this stage a secondary pump could then be used to advance the ozonide solution through the previously developed resin-quenching process. This setup was readily achieved and successfully used to process larger quantities of material. Another useful feature of this setup was the very small stoichiometric excess of ozone required, ranging from only 1.5−2 equiv. Under optimized conditions it was possible to achieve a throughput of 6.6 g/h, equating to over 200 g of product per day when processing in a continuous fashion.

Having access to gram quantities of the azalactone intermediates **16a/b** we evaluated their reactivity as coupling agents via reaction with various nitrogen nucleophiles (Figure 18, Table 3).[30] This proved an exceedingly viable trans-

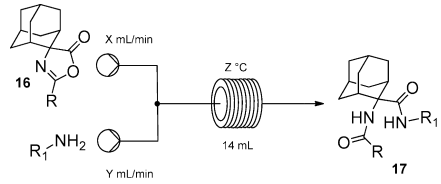

Figure 18. Flow reactions of azalactones **16a/b** with nitrogen nucleophiles.

formation, giving high yields of the coupled material following only direct filtration of the reactor output to isolate the solid product.

Synthetic Step 5: Hydrolytic Cleavage. Our initial starting point for comparison purposes with the batch process was the conditions developed by Edward et al. for the hydrolytic cleavage of benzamide **9** (Scheme 2).[15d] By applying these conditions, the phenyl derivative **16b** was quantitatively

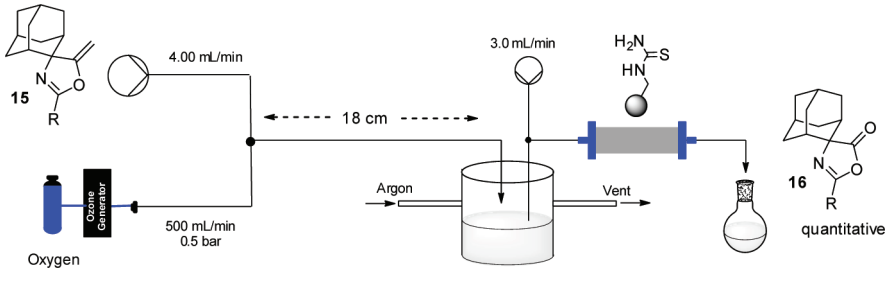

Figure 17. PTFE reactor-tube for ozonolysis in the optimized flow conditions.

dx.doi.org/10.1021/op300084z | Org. Process Res. Dev. 2012, 16, 798−810

Table 3. Flow reactions of azalactones 16a/b with nitrogen nucleophiles

	R	R_1	Flow rate mL min^{-1}	Temp °C	Solvent	Yield %
17a	Ph		1.0	60	THF	Quant.
17b	Ph		0.5	60	THF	Quant.
17c	Ph		0.4	100	MeCN	Quant.
17d	Ph		0.5	60	THF	Quant.
17e	Ph		0.3	100	THF	89
17f	Ph		0.3	100	MeCN	91
17g	Ph		0.2	130	PBS,[a] CH_3CN 1:3 *v/v*	78
17h	Ph		0.5	60	THF	Quant.
17i	Ph	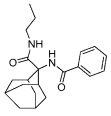	0.3	100	MeCN	Quant.
17j	Ph		0.2	130	PBS[a], CH_3CN 1:3 *v/v*	65
17k	Ph		0.25	130	PBS[a], CH_3CN 1:3 *v/v*	70
17l	Ph		0.3	60	THF	Quant.
17m	Me	CH_3-, CH_3O-	0.25	100	PBS[a], CH_3CN 1:3 *v/v*	75
17n	Me		1.0	60	THF	Quant.

[a]PBS = phosphate buffered saline, pH 7.4; Sigma Aldrich cat. no. P4417-100TAB.

converted to the corresponding amino acid **1** after 80 h at reflux in 70% isolated yield on a 10 mmol scale. A much faster reaction was observed for the corresponding methyl derivative **16a** which required only 28 h (96% isolated yield). Furthermore, the workup for the amino acid **1** from the simple acyl analogue, compound **16a**, was far easier due to the volatility of the displaced acetic acid as opposed to the resulting benzoic acid generated from **16b**. However, in each case the product obtained as its hydrochloride salt was a perfect match for the authentic material previously prepared and purified (Schemes 1 and 2).

We therefore proceeded to transpose the general hydrolysis procedure to flow. Our test setup employed two injection loops (3 mL), one loaded with the azalactone **16** in acetic acid and the other containing a mixture of $AcOH/H_2O/HCl$, 9:1.8:1 (v/v/v). The two channels were simultaneously switched into the main flow stream of AcOH/HCl, 40:1 (v/v) and combined at a T-piece before progressing into a 14 mL PFA CFC. Again, temperature was found to be a principle parameter; reaction temperatures below 130 °C gave substantial quantities of the *N*-acylamino acid derivatives **18** and **9** (Figure 19). Likewise increasing the flow rate beyond 0.80 mL min^{-1} per channel (residence time 9 min) gave incomplete hydrolysis, resulting in quantitative isolation of **18** and **9**.

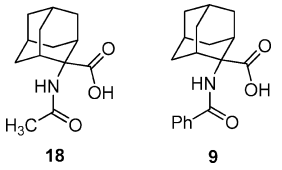

Figure 19. *N*-Acylamino acid formed during low-temperature processing.

The final optimized conditions used for scale-up involved processing a solution of azalactone **16** in AcOH continuously introduced to the system at a fixed flow rate (0.40 mL min^{-1} for **16a** and 0.25 mL min^{-1} for **16b**, equating to residence times of 18 and 28 min, respectively) to unite at a standard-T connector with a solution of $HCl/AcOH/H_2O$ (9:1.8:1 [v/v/v] equal flow rate). The combined solution was then directed into a 14 mL PFA CFC heated at an elevated temperature of 150 °C (Figure 20). The exiting reaction mixture was collected and

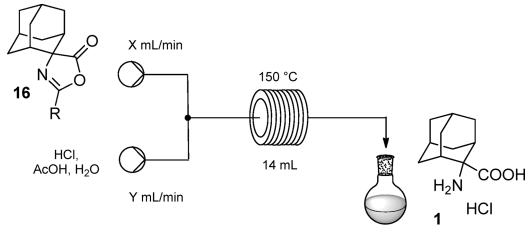

16a → **1** R = Me (yield 94%), X = 0.40 and Y = 0.40 mL min^{-1}
16b → **1** R = Ph (yield 87%), X = 0.25 and Y = 0.25 mL min^{-1}

Figure 20. Flow conditions for the hydrolytic deprotection to amino acid **1**.

concentrated in vacuo to obtain an off-white solid which was triturated with hot Et_2O. Bulk recrystallization from methanol (0 °C, overnight), gave 2-aminoadamantane-2-carboxylic acid (**1**) as the hydrochloride salt in very good yield (94% from **16a** and 87% from **16b**). Under these optimized conditions a throughput of 4.4 g of product (**16a**) per day (2.75 g for **16b**) could be realized using a single coil reactor unit which can be easily run in a parallel reactor setup multiplying the output.

■ CONCLUSIONS

In summary, we have developed a multistep sequence to the title aminoacid **1** which utilizes flow-based reactor technology to aid in the preparation and facilitate scale-up of the sequence. The isolation at each stage of the process has been achieved without recourse to column chromatography, in high yield and giving quality material ready for telescoping into the subsequent step. An overall yield for the route to the methyl derivative **16a** of 76% was achieved, whereas a slightly lower final yield of 70% was attained for the phenyl derivative **16b**. The equipment used for the processing can be easily attained from commercial suppliers or, in the case of the self-assembled

dx.doi.org/10.1021/op300084z | *Org. Process Res. Dev.* 2012, 16, 798−810

reactors, rapidly constructed without a high level of engineering skill. We have found this approach to be highly amenable to laboratory-based scale-up of this amino acid structure and has allowed us to reproducibly generate several hundred grams of final product.

EXPERIMENTAL SECTION

General Experimental Section. ^{1}H NMR spectra were recorded on a Bruker Avance DPX-400 spectrometer with the residual solvent peak as the internal reference ($CDCl_3$ = 7.26 ppm, d_6-DMSO = 2.50 ppm). ^{1}H resonances are reported to the nearest 0.01 ppm. ^{13}C NMR spectra were recorded on the same spectrometers with the central resonance of the solvent peak as the internal reference ($CDCl_3$ = 77.16 ppm, d_6-DMSO = 39.52 ppm). All ^{13}C resonances are reported to the nearest 0.1 ppm. DEPT 135, COSY, HMQC, and HMBC experiments were used to aid structural determination and spectral assignment. The multiplicity of ^{1}H signals are indicated as: s = singlet, d = doublet, t = triplet, m = multiplet, br = broad, or combinations of thereof. Coupling constants (J) are quoted in hertz (Hz) and reported to the nearest 0.1 Hz. Where appropriate, averages of the signals from peaks displaying multiplicity were used to calculate the value of the coupling constant. Infrared spectra were recorded neat on a PerkinElmer Spectrum One FT-IR spectrometer using Universal ATR sampling accessories. Letters in parentheses refer to the relative absorbency of the peak: w = weak, less than 40% of the most intense peak; m = medium, ∼41−69% of the most intense peak; s = strong, greater than 70% of the most intense peak. Unless stated otherwise, reagents were obtained from commercial sources and used without purification. Laboratory reagent grade EtOAc, petroleum ether 40−60, and DCM were obtained from Fischer Scientific and distilled before use. Unless stated otherwise, heating was conducted using standard laboratory apparatus. The removal of solvent under reduced pressure was carried out on a standard rotary evaporator, a Genevac EZ-2 Plus personal evaporator, or a Vapourtec V-10 evaporator. Melting points were performed on a Stanford Research Systems MPA100 (OptiMelt) automated melting point system and are uncorrected. High-resolution mass spectrometry (HRMS) was performed using a Waters Micromass LCT Premier spectrometer using time-of-flight with positive ESI, or conducted by Mr. Paul Skelton on a Bruker BioApex 47e FTICR spectrometer using positive ESI or EI at 70 eV to within a tolerance of 5 ppm of the theoretically calculated value. LC−MS analysis was performed on an Agilent HP 1100 series chromatography (Mercury Luna 3u C18 (2) column) attached to a Waters ZQ2000 mass spectrometer with ESCi ionization source in ESI mode. Elution was carried out at a flow rate of 0.6 mL min^{-1} using a reverse-phase gradient of acetonitrile and water containing 0.1% formic acid. Retention time (R_t) is given in min to the nearest 0.1 min, and the m/z value is reported to the nearest mass unit (m.u.). X-ray crystal structures were determined by Dr. John Davies at the Department of Chemistry, University of Cambridge. CIF numbers are reported as part of compound characterization. Elemental analyses within a tolerance of ±0.3% of the theoretical values were determined by Mr. Alan Dickerson and Mrs. Patricia Irele in the microanalytical laboratories at the Department of Chemistry, University of Cambridge.

Additional experimental procedures and full compound characterizations are contained within the Supporting Information.

Flow Synthesis of Amino Acid 1 (General Figure 5). 2-Ethynyl Adamantan-2-ol (13). See Figure 8. A solution of 2-adamantanone (**5**) (100.0 g, 660 mmol, 0.5 M in THF, flow rate 0.18 mL min^{-1}, pump A) and a solution of ethynyl magnesium bromide (0.5 M in THF, flow rate 0.20 mL min^{-1}, pump B) were combined at a T-piece using a Uniqsis Flowsyn (residence time 37 min) and passed through a 14 mL PFA CFC heated at 40 °C. After exiting the CFC the flow stream was quenched with a saturated solution of NH_4Cl solution (flow rate 0.18 mL min^{-1}, pump C) mixed at a second T-piece. The T-piece was sonicated to avoid blockages due to formation of insoluble magnesium salts. The combined biphasic output was collected, and the two phases were separated; the water phase was washed once with Et_2O, and then the organic solution obtained was dried over sodium sulfate. Evaporation of the solvent and subsequent crystallization from hexane furnished the desired product 2-ethynyl adamantan-2-ol (**13**) as a white solid (105.5 g, 590 mmol, yield 90%, mp 101.7 °C); LC−MS: retention time 4.63 min, m/z $[M + H]^{dehydrated}$ = 159.00. FT-IR (neat, cm^{-1}) ν: 3366 (m), 3181 (m), 2898 (m), 2159 (w), 754 (m); ^{1}H NMR (400 MHz, $CDCl_3$): δ/ppm = 2.53 (s, 1H), 2.18−2.13 (m, 4H), 1.96−1.96 (m, 3H), 1.82−1.77 (m, 4H), 1.70 (br s, 2H), 1.55−1.58 (m, 3H). ^{13}C NMR (100 MHz, $CDCl_3$): δ/ppm = 88.51 (C), 72.70 (C_{sp}−H), 72.50 (C), 39.31 (CH), 37.60 (CH_2), 35.37 (CH_2), 31.54 (CH_2), 26.40 (CH), 26.23 (CH). HRMS: calculated for $[C_{12}H_{17}O]^+$ 177.2550, found 177.2558.

2-Ethynyl-2-acetamido Adamantane (14a). See Figure 8. *Expt A (small scale).* A solution of 2-ethynyl adamantan-2-ol (**13**) (0.3 g, 1.7 mmol), MeCN (1.6 mL), and AcOH (2 mL), loaded in a 3 mL injection loop (A), and neat conc. sulfuric acid (3 mL), loaded in a 3 mL injection loop (B), were simultaneously switched into the main flow stream of glacial acetic acid/acetic anhydride, 10:1 (v/v) (flow rate of 1.00 mL min^{-1} per channel) combining at a T-piece before progressing into a 14 mL PFA CFC heated at 30 °C (residence time 7 min). After exiting the CFC this flow stream was quenched with a third stream containing KOH solution (3 M, pump C at a flow rate 3 mL min^{-1}), and the salts formed were filtered and washed with DCM. After separation of the two phases the organic layer was dried over sodium sulfate and concentrated to obtain a crude material that after trituration with hexane gave the title compound (**14a**) as a white solid (0.3 g, 1.4 mmol, yield 86%);

Expt B (scale-up). A solution of 2-ethynyl adamantan-2-ol (**13**) (20.0 g, 113.6 mmol, pump A), MeCN (80 mL), and AcOH (88 mL) and a mixture of conc. sulfuric acid (40 mL, pump B), acetic acid (88 mL), and acetic anhydride (40 mL) were pumped using a Uniqsis Flowsyn at a flow rate of 1.00 mL min^{-1} per channel (residence time 7 min) through a 14 mL PFA CFC heated at 30 °C. After exiting the CFC this flow stream was quenched with a third stream containing KOH solution (3 M, pump C at a flow rate 3 mL min^{-1}), and the salts formed were filtered and washed with DCM. After separation of the two phases the organic layer was dried over sodium sulfate and concentrated to obtain a crude material that after trituration with hexane gave the title compound (**14a**) as a white solid (21.8 g, 99.0 mmol, yield 91%, mp 147 °C); LC−MS: retention time 4.39 min, m/z [M + H] = 218.14. FT-IR (neat, cm^{-1}) ν: 3287 (m), 2903 (m), 2166 (w), 1645 (s), 1537 (s), 670 (m); ^{1}H NMR (400 MHz, $CDCl_3$): δ/ppm = 5.41 (br s, 1H), 2.46 (s, 1H), 2.40 (br s, 2H), 2.35 (br s, 1H), 2.31 (br s, 1H), 2.01 (s, 3H), 1.82−1.77 (m, 4H), 1.70 (br s, 2H), 1.55−

dx.doi.org/10.1021/op300084z | Org. Process Res. Dev. 2012, 16, 798−810

1.58 (m, 3H). ^{13}C NMR (400 MHz, $CDCl_3$): δ/ppm = 169.12 (C), 86.18 (C), 71.73 (C_{sp}–H), 56.47 (C), 37.64 (CH_2), 35.06 (CH), 34.37 (CH_2), 32.18 (CH_2), 27.24 (CH), 26.76 (CH), 24.23 (CH_3). HRMS: calculated for $[C_{14}H_{20}NO]^+$ 218.1545, found 218.1548.

2-Ethynyl-2-benzamido Adamantane (14b). See Figure 10. *EXPT A (small scale).* A solution of 2-ethynyl adamantan-2-ol (**13**) (0.3 g, 1.7 mmol), benzonitrile (0.8 mL, 7.8 mmol, 4.6 equiv) and AcOH (2.1 mL), loaded in a 3 mL injection loop (A), and neat conc. sulfuric acid (3 mL), loaded in a 3 mL injection loop (B), were simultaneously switched into the main flow stream of glacial acetic acid/acetic anhydride, 10:1 (v/v) (flow rate of 1.00 mL min^{-1} per channel) combining at a T-piece before progressing into a 14 mL PFA-CFC heated at 30 °C (residence time 7 min). After exiting the CFC this flow stream was quenched with a third stream containing KOH solution (3 M, pump C at a flow rate 3 mL min^{-1}), and the salts formed were filtered and washed with DCM. After separation of the two phases the organic layer was dried over sodium sulfate and concentrated to obtain a crude material that after trituration with hexane gave the title compound (**14b**) as a white solid (0.38 g, 1.3 mmol, yield 77%);

EXPT B (scale-up). A solution of 2-ethynyl adamantan-2-ol (**13**) (50.0 g, 280 mmol, pump A), benzonitrile (98 mL, 0.95 mol, 3.4 equiv) and acetic acid (196 mL) and a mixture of concentrated sulfuric acid (98 mL, pump B), acetic acid (215 mL) and acetic anhydride (98 mL) were pumped using a Uniqsis FlowSyn at a flow rate of 1.00 mL min^{-1} per channel (residence time 7 min) through a 14 mL PFA CFC maintained at 30 °C. After exiting the CFC this flow stream was quenched with 3 M aqueous KOH solution (pump C, flow rate 3 mL min^{-1}) and the salts formed were filtered off and washed with DCM. After separation of the phases the organic phase is dried over sodium sulfate and concentrated to obtain a crude, oily material that after trituration with hexane gave the title compound (**14b**) as white solid (50.1 g, 174 mmol, yield 64%).

EXPT C (scale-up modified conditions). A solution of 2-ethynyl adamantan-2-ol (**13**) (50.0 g, 0.28 mol, pump A), benzonitrile (49 mL, 0.475 mol, 1.7 equiv) and acetic acid (196 mL) and a mixture of concentrated sulfuric acid (98 mL, pump B), acetic acid (215 mL) and acetic anhydride (98 mL) were pumped using a Uniqsis FlowSyn at a flow rate of 0.60 mL min^{-1} per channel (residence time 11.6 min) through a 14 mL PFA CFC maintained at 30 °C. After exiting the CFC this flow stream was quenched with 3 M aqueous KOH solution (pump C, flow rate 1.8 mL min^{-1}) and the salts formed were filtered off washing with DCM. After separation of the phases the organic one is dried over sodium sulfate and concentrated to obtain a crude oily material that after trituration with hexane gave the title compound (**14b**) as white needles (66.5 g, 231 mmol, yield 85%, mp 189 °C); LC–MS: retention time 4.98 min, m/z [M + H] = 280.15. FT-IR (neat, cm^{-1}) ν: 3400 (m), 3281 (m), 2905 (m), 1645 (s), 1537 (s), 690 (s); ^{1}H NMR (400 MHz, $CDCl_3$): δ/ppm = 7.96 (d, 2H, J = 6.8 Hz), 7.49 (m, 1H), 7.40 (m, 2H), 6.14 (br s, 1H), 2.56 (s, 2H), 2.49 (s, 1H), 2.40 (d, 2H, J = 11.2 Hz), 2.00 (d, 2H, J = 11.2 Hz), 1.89–1.70 (m, 9H). ^{13}C NMR (100 MHz, $CDCl_3$): δ/ppm = 166.26 (C), 135.27 (C), 131.47 (CH), 128.60 (CH), 126.94 (CH), 86.04 (C), 71.99 (C_{sp}–H), 56.63 (C), 37.66 (CH_2), 35.28 (CH), 34.06 (CH_2), 32.01 (CH_2), 26.92 (CH), 26.48 (CH). HRMS: calculated for $[C_{19}H_{22}NO]^+$ 280.1701, found 280.1691.

2-Methyl-4-(adamantane-2′-spiro)-5-methylidene Oxazoline (15a). See Figure 12. A solution of 2-ethynyl 2-acetylamino adamantane (**14a**) (9.0 g, 41.3 mmol, flow rate 0.20 mL min^{-1}, pump A) in EtOH (400 mL) and a solution of potassium hydroxide (13.0 g, flow rate 0.10 mL min^{-1}, pump B) in EtOH (200 mL) were pumped using a Uniqsis Flowsyn (residence time 47 min) through a 14 mL PFA CFC heated at 125 °C using a 100 psi BPR. After exiting the CFC this flow stream was collected and the solution concentrated in vacuo. The solid obtained was quenched with distilled water (ice bath to avoid any retroreaction) and extracted with DCM. After drying over sodium sulfate, the solvent was evaporated and the title compound (**15a**) isolated as a yellowish solid (8.2 g, 37.6 mmol, yield 91%, mp 61.5 °C).

*Telescoped Procedure for the Synthesis of Oxazolines (**15a**). See Figure 13.* A solution of 2-ethynyl adamantan-2-ol (**13**) (2.0 g, 11 mmol, pump A), MeCN (8.0 mL), and AcOH (9 mL) and a mixture of conc sulfuric acid (4.0 mL, pump B), acetic acid (9 mL), and acetic anhydride (4.0 mL) was pumped using a Uniqsis Flowsyn at a flow rate of 1.00 mL min^{-1} per channel (residence time 7 min) through a 14 mL PFA CFC heated at 30 °C. After exiting the CFC the flow stream was directed to a T-piece to meet a further solution of KOH (3 M) in EtOH/H_2O, 40:1 (v/v) (pump C, flow rate 3.0 mL min^{-1}) and then filtered in-line (column packed with glass wool) to remove any precipitate (eluent collected in a filter flask). The resultant solution was pumped into a PFA CFC and heated to 120 °C (residence time 48 min, flow rate 0.30 mL min^{-1}). After exiting the CFC the flow stream was collected and the solution concentrated in vacuo. The solid obtained was quenched with distilled water (ice bath to avoid any retroreaction), extracted with DCM, and dried over sodium sulfate, and the solvent was evaporated. The title compound (**15a**) was obtained as a yellowish solid (2.2 g, 10 mmol, yield 91%). LC–MS: retention time 3.70 min, m/z $[M + H]^{protonated}$ = 219.05; time 4.49 min, m/z [M + H] = 218.07. FT-IR (neat, cm^{-1}) ν: 2906 (s), 1686 (s), 1654 (s), 1262 (s), 1199 (s), 1063 (s), 965 (s), 834 (s). ^{1}H NMR (400 MHz, $CDCl_3$): δ/ppm = 4.79 (d, 1H, J = 2.4 Hz), 4.52 (d, 1H, J = 2.4 Hz), 2.44 (d, 2H, J = 12.4 Hz), 2.21 (d, 2H, J = 12.4 Hz), 2.03 (s, 3H), 1.86 (br s, 3H), 1.74 (s, 2H), 1.69–1.55 (m, 5H). ^{13}C NMR (100 MHz, $CDCl_3$): δ/ppm = 166.00 (C), 158.66 (C), 87.91 (CH_2), 76.02, 38.70 (CH_2), 37.08 (CH), 34.06 (CH_2), 31.40 (CH_2), 28.03 (CH), 26.76 (CH), 14.43 (CH_3). HRMS: calculated for $[C_{14}H_{20}NO]^+$ 218.1545, found 218.1541. The structure was unambiguously confirmed by single X-ray crystallography and deposited at Cambridge University (Crystallographic Data Centre) with the unique reference CCDC860429; space group $P21/c$; a = 6.6834 (2) Å, b = 7.0945 (2) Å, c = 23.8587 (8) Å, β = 90.449 (2)°.

2-Phenyl-4-(adamantane-2′-spiro)-5-methylidene Oxazoline (15b). See Figure 12. A solution of 2-ethynyl 2-benzamido adamantane (**14b**) (17.5 g, 63 mmol, flow rate 0.40 mL min^{-1}, pump A) in EtOH (800 mL) and a solution of potassium hydroxide (20.0 g, flow rate 0.20 mL min^{-1}, pump B) in EtOH (400 mL) were pumped using a Uniqsis Flowsyn (residence time 24 min) through a 14 mL PFA CFC heated at 120 °C using a 100 psi BPR. After exiting the CFC this flow stream was collected and the solution concentrated in vacuo. The solid obtained was quenched with distilled water (ice bath to avoid any retroreaction) and extracted with DCM. After drying over sodium sulfate and evaporating the solvent, the title compound (**15b**) was obtained as a yellowish solid (16.2 g, 53 mmol, yield 92%, mp 67 °C).

dx.doi.org/10.1021/op300084z | Org. Process Res. Dev. 2012, 16, 798–810

*Telescoped Procedure for the Synthesis of Oxazolines (**15b**). See Figure 13.* A solution of 2-ethynyl adamantan-2-ol (**13**) (5.0 g, 28 mmol, pump A), benzonitrile (4.9 mL, 47.5 mmol, 1.7 equiv), and acetic acid (20 mL) and a mixture of concentrated sulfuric acid (9.8 mL, pump B), acetic acid (21.5 mL), and acetic anhydride (9.8 mL) was pumped using a Uniqsis FlowSyn at a flow rate of 0.60 mL min^{-1} per channel (residence time 11.6 min) through a 14 mL PFA CFC maintained at 30 °C. After exiting the CFC the flow stream was directed to a T-piece to meet a further solution of KOH (3 M) in EtOH/H_2O, 40:1 (v/v) (pump C, flow rate 1.8 mL min^{-1}) then filtered in-line (column packed with glass wool) to remove any precipitate (eluent collected in a filter flask). The resultant solution was pumped into a PFA CFC and heated to 120 °C (residence time 24 min, flow rate 0.60 mL min^{-1}). After exiting the CFC the flow stream was collected and the solution concentrated in vacuo. The solid obtained was quenched with distilled water (ice bath to avoid any retroreaction), extracted with DCM, and dried over sodium sulfate, and the solvent was evaporated. The title compound (**15b**) was obtained as a yellowish solid (7.0 g, 25 mmol, yield 90%). LC−MS: retention time 6.05 min, m/z [M + H] = 280.08. FT-IR (neat, cm^{-1}) ν: 2899 (s), 1666 (s), 1644 (s), 1056 (s). ^{1}H NMR (400 MHz, $CDCl_3$): δ/ppm = 8.01 (d, 2H, J = 6.8 Hz), 7.49−7.40 (m, 3 H), 4.99 (d, 1H, J = 2.4 Hz), 4.65 (d, 1H, J = 2.4 Hz), 2.63 (d, 2H, J = 11.2 Hz), 2.29 (d, 2H, J = 11.2 Hz), 1.95 (m, 2H), 1.74 (s, 2H), 1.69−1.55 (m, 6H). ^{13}C NMR (100 MHz, $CDCl_3$): δ/ppm = 166.04 (C), 157.63 (C), 131.98 (CH), 128.81 (CH), 128.12 (CH), 126.97, 88.45 (CH_2), 77.14, 38.73 (CH_2), 37.68 (CH), 34.14 (CH_2), 31.51 (CH_2), 27.96 (CH), 26.54 (CH). HRMS: calculated for $[C_{19}H_{22}NO]^+$ 280.1701, found 218.1704. The structure was unambiguously confirmed by single X-ray crystallography and deposited at Cambridge University (Crystallographic Data Centre) with the unique reference CCDC860430; space group *Pbca*: a = 20.3254 (3) Å, b = 12.2093 (1) Å, c = 23.7513 (3) Å.

2-Methyl-4-(adamantane-2′-spiro)-oxazolin-5-one (16a). See Figure 17. A solution of 2-methyl-4-(adamantane-2′-spiro)-5-methylidene oxazoline (**15a**) (9.0 g, 41.3 mmol, flow rate 4.00 mL min^{-1}, pump A) in DCM (400 mL), and a stream of ozone (0.5 bar, flow rate 500 mL min^{-1}) were combined in a T-piece and directly through a 1 mL PTFE tube reactor (180 mm, 2.5 mm i.d., ∼15 s residence time). After exiting the tube this flow stream was collected, and the excess of ozone was blown out with argon. The solution was then directly delivered to a scavenger cartridge containing QP-TU (3.00 mL min^{-1}, pump B). The collection of the output stream and the concentration of the solution gave the title compound (**16a**) as a white solid (8.7 g, 39.4 mmol, yield 95%, mp 138 °C); LC−MS: retention time 4.32 min, m/z $[M + H]^{decarboxylated}$ = 192.09, m/z $[M - H]^{acid}$ = 236.07. FT-IR (neat, cm^{-1}) ν: 2907 (s), 1789 (m), 1693 (s), 1448 (m), 1232 (s), 1174 (s), 1046 (s), 971 (s), 900 (s). ^{1}H NMR (400 MHz, $CDCl_3$): δ/ppm = 2.51 (d, 2H, J = 12 Hz), 2.35 (d, 2H, J = 11.2 Hz), 2.19 (s, 3H), 1.94 (s, 2H), 1.71−1.60 (m, 8H). ^{13}C NMR (100 MHz, $CDCl_3$): δ/ppm = 179.12 (C), 159.27 (C), 72.28 (C), 37.79 (CH_2), 35.04 (CH), 33.61 (CH_2), 31.09 (CH_2), 27.48 (CH), 26.31 (CH), 15.33 (CH_3). HRMS: calculated for $[C_{13}H_{18}NO_2]^+$ 220.1339, found 220.1347. The structure was unambiguously confirmed by single X-ray crystallography and deposited at Cambridge University (Crystallographic Data Centre) with the unique reference CCDC860432; space group *P*21/*m*: a = 6.8926 (4) Å, b = 6.5463 (4) Å, c = 12.267 (2) Å, β = 98.997 (2)°.

2-Phenyl-4-(adamantane-2′-spiro)-oxazolin-5-one (16b). See Figure 17. A solution of 2-phenyl-4-(adamantane-2′-spiro)-5-methylidene oxazoline (**15b**) (10.0 g, 35.8 mmol, flow rate 4.00 mL min^{-1}, pump A) in DCM (350 mL) and a stream of ozone (0.5 bar, flow rate 500 mL min^{-1}) were combined in a T-piece and directly through a 1 mL PTFE tube reactor (180 mm, 2.5 mm i.d., ∼15 s residence time). After exiting the tube this flow stream was collected and the excess of ozone was blown out with argon. The solution was then directly delivered to a scavenger cartridge containing QP-TU (3.00 mL min^{-1}, pump B). The collection of the output stream and the concentration of the solution gave the title compound (**16b**) as a white solid (10.09 g, 35.7 mmol, yield 99.8%, mp 109 °C); LC−MS: retention time 5.64 min, m/z $[M + H]^{decarboxylated}$ = 254.12, m/z $[M - H]^{acid}$ = 298.05. FT-IR (neat, cm^{-1}) ν: 2893 (s), 1796 (s), 1657 (s), 1453 (m), 1292 (s), 1046 (s), 961 (s), 678 (s). ^{1}H NMR (400 MHz, $CDCl_3$): δ/ppm = 8.03 (d, 2H, J = 6.8 Hz), 7.55−7.51 (m, 1H), 7.49−745 (m, 2H), 2.59 (d, 2H, J = 14 Hz), 2.54 (d, 2H, J = 14 Hz), 1.99 (s, 2H), 1.87 (s, 2H), 1.82 (2, 2H), 1.70 (m, 4H). ^{13}C NMR (100 MHz, $CDCl_3$): δ/ppm = 179.04 (C), 157.96 (C), 132.25 (CH), 128.68 (CH), 127.87 (CH), 126.64 (C), 72.79 (C), 37.81 (CH_2), 35.51 (CH), 33.67 (CH_2), 31.20 (CH_2), 27.67 (CH), 26.39 (CH). HRMS: calculated for $[C_{18}H_{20}NO_2]^+$ 282.1494, found 218.1484. The structure was unambiguously confirmed by single X-ray crystallography and deposited at Cambridge University (Crystallographic Data Centre) with the unique reference CCDC860431; space group *P*21/*m*: a = 12.6229 (9) Å, b = 6.9172 (5) Å, c = 17.039 (2) Å, β = 109.380 (3)°.

2-Aminoadamantane-2-carboxylic Acid Hydrochloride (1). See Figure 20. *Expt A.* A solution of 2-methyl-4-(adamantane-2′-spiro)-oxazolin-5-one (**16a**) (1.15 g, 5.25 mmol, flow rate 0.40 mL min^{-1}, pump A) in glacial acetic acid (150 mL) and a mixture of glacial acetic acid (90 mL), H_2O (50 mL), and hydrochloric acid (10 mL, flow rate 0.40 mL min^{-1}, pump B) were combined in a T-piece and reacted through a 14 mL PFA reactor coil at 150 °C (residence time ∼18 min). After exiting the tube this flow stream was collected, and the mixture was concentrated in vacuo. The solid obtained was washed with hot diethyl ether (50 mL × 2) and hot acetonitrile (50 mL × 2) to obtain the product that was crystallised from methanol (1.10 g, 4.8 mmol, yield 94%).

Expt B. A solution of 2-phenyl-4-(adamantane-2′-spiro)-oxazolin-5-one (**16b**) (1.50 g, 5.25 mmol, flow rate 0.25 mL min^{-1}, pump A) in glacial acetic acid (150 mL) and a mixture of glacial acetic acid (90 mL), H_2O (50 mL), and hydrochloric acid (10 mL) (flow rate 0.25 mL min^{-1}, pump B) were combined in a T-piece and reacted through a 14 mL PFA reactor coil at 150 °C (residence time ∼28 min). After exiting the tube this flow stream was collected, and the mixture was concentrated in vacuo. The solid obtained was washed with hot diethyl ether (50 mL × 2) and hot acetonitrile (50 mL × 2) to obtain the product that was crystallised from methanol (1.05 g, 4.55 mmol, yield 87%, mp >258 °C decomposition); LC−MS: retention time 0.31 min, m/z $[M + H]^{decarboxylated}$ = 149.99, m/z $[M + H]^{deaminated}$ = 179.05, m/z [M + H] = 196.10, m/z [M − H] = 194.06. FT-IR (neat, cm^{-1}) ν: 3220 (w), 3168 (w), 2775 (s), 1725 (s), 1587 (s), 1506 (s), 1468 (s); ^{1}H NMR (400 MHz, $CDCl_3$): δ/ppm = 8.70 (s br, 3H), 2.21 (s, 2H), 2.12 (d, 2H, J = 13.2 Hz), 1.92 (d, 2H, J = 13.2 Hz), 1.75−1.80 (m,

dx.doi.org/10.1021/op300084z | *Org. Process Res. Dev.* 2012, 16, 798−810

4H), 1.62−1.66 (m, 2H). ^{13}C NMR (100 MHz, $CDCl_3$): δ/ppm = 171.59 (C), 63.92 (C), 37.54 (CH_2), 34.40 (CH), 32.24 (CH_2), 31.22 (CH), 26.28 (CH). HRMS: calculated for $[C_{11}H_{18}NO_2]^+$ 196.1338, found 196.1336. Microanalysis calculated (found) for $C_{11}H_{18}NO_2Cl$: C 57.02 (56.90%), H 7.83 (7.97%), N 6.04 (6.06%). The structure was unambiguously confirmed by X-ray crystallography and deposited at Cambridge University (Crystallographic Data Centre) with the unique reference CCDC860428; space group $P21/c$: a = 6.3862 (2) Å, b = 11.4838 (3) Å, c = 14.9079 (4) Å, β = 95.392 (2)°.

*Characterisation of Partial Hydrolysis Products from **16a** and **16b**. 2-Acetylamido Adamantane-2-carboxylic Acid (**18**).* Off-white solid; mp 210−213 °C; LC−MS: retention time 4.06 min, m/z [M − H] = 236.10. FT-IR (neat, cm^{-1}) ν: 3386 (m), 2907 (s), 1745 (s), 1632 (m), 1594 (s), 1248 (s), 1208 (s), 849 (m), 721 (m); ^{1}H NMR (400 MHz, $CDCl_3$): δ/ppm = 12.01 (br s, 1H), 7.62 (s, 1H), 2.39 (s, 2H), 2.01 (brs, 4H), 1.82 (s, 3H), 1.73 (s, 2H), 1.62 (br s, 4H), 1.49 (m, 2H). ^{13}C NMR (100 MHz, $CDCl_3$): δ/ppm = 174.18 (C), 169.44 (C),63.10 (C), 38.02 (CH_2), 35.80 (CH), 32.50 (CH_2), 32.01 (CH_2), 26.99 (CH), 26.71 (CH), 23.40 (CH_3). HRMS: calculated for $[C_{13}H_{20}NO_3]^+$ 238.1718, found 238.1710. The structure was unambiguously confirmed by X-ray crystallography and deposited at Cambridge University (Crystallographic Data Centre) with the unique reference CCDC 874390; space group $P\bar{1}$: a = 6.8572 (2) Å, b = 8.1043 (3) Å, c = 10.8425 (5) Å; α = 90.434(2)°, β = 102.620(2)°, γ = 98.459(3)°.

*2-Benzamido Adamantane-2-carboxylic Acid (**9**).* Off-white solid; mp 234−236 °C; LC−MS: retention time 4.28 min, m/z $[M + H]^+$ = 322.14. FT-IR (neat, cm^{-1}) ν: 3389.7 (w), 2905.7 (m), 1740.0 (s), 1626.8 (m), 1526.3 (s); ^{1}H NMR (400 MHz, d_6-DMSO): δ/ppm = 12.17 (br s, 1H), 8.10 (s, 1H), 7.79 (d, 2H, J = 7.2 Hz), 7.52 (t, 1H, J = 7.2 Hz), 7.44 (t, 2H, J = 7.2 Hz), 2.63 (s, 2H), 2.12 (m, 4H), 1.80 (s, 2H), 1.65−1.69 (m, 4H), 1.56 (d, 2H, J = 12.7 Hz); ^{13}C NMR (100 MHz, d_6-DMSO): δ/ppm = 173.8, 166.4, 135.1, 131.1 (CH), 128.1 (CH), 127.7 (CH), 63.1, 37.5 (CH), 33.5 (CH_2), 32.8 (CH_2), 31.5 (CH_2), 26.5 (CH), 26.4 (CH); HRMS: calculated for $[C_{18}H_{21}NO_3Na]^+$ 322.1419, found 322.1421. The structure was unambiguously confirmed by X-ray crystallography and deposited at Cambridge University (Crystallographic Data Centre) with the unique reference CCDC 860427; space group $P21/n$: a = 14.1635 (4) Å, b = 6.7026 (2) Å, c = 15.8379 (6) Å, β = 99.395 (1)°.

■ ASSOCIATED CONTENT

Ⓢ Supporting Information

This material is available free of charge via the Internet at http://pubs.acs.org.

■ AUTHOR INFORMATION

Corresponding Author

*theitc@ch.cam.ac.uk

Notes

The authors declare no competing financial interest.

■ ACKNOWLEDGMENTS

We thank the Royal Society (I.R.B.), "Sapienza" University of Rome (C.B.) and the BP endowment (S.V.L.) for financial support. We also wish to thank Dr. J. E. Davies for crystal structure determination and the EPSRC for a financial contribution toward the purchase of the X-ray diffractometer.

■ REFERENCES

(1) (a) Maison, W.; Frangioni, J. V.; Pannier, N. *Org. Lett.* **2004**, *24*, 4567−4569. (b) Papanastasiou, I.; Foscolos, G. B.; Tsotinis, A.; Olah, J.; Ovadi, J.; Prathalingam, S. R.; Kelly, J. M. *Heterocycles* **2008**, *75*, 2043−2061. (c) Lamoureux, G.; Artavia, G. *Curr. Med. Chem.* **2010**, *17*, 2967−2978.

(2) Liu, J.; Obando, D.; Liao, V.; Lifa, T.; Codd, R. *Eur. J. Med. Chem.* **2011**, *46*, 1949−1963.

(3) (a) Nagasawa, H. T.; Elberling, J. A.; Shirota, F. N. *J. Pharm. Sci.* **1980**, *69*, 1022−1025. (b) Kovtun, V. Y.; Plakhotnik, V. M. *Pharm. Chem. J* **1987**, *21*, 555−563. (c) Knijnenburg, A. D.; Kapoerchan, V. V.; Spalburg, E.; de Neeling, A. J.; Mars-Groenendijk, R, H.; Noort, D.; van der Marel, G. A.; Overkleeft, H. S.; Overhand, M. *Bioorg. Med. Chem.* **2010**, *18*, 8403−8409.

(4) (a) Hong, F.; Zaidi, J.; Cusack, B.; Richelson, E. *Bioorg. Med. Chem.* **2002**, *10*, 3849−3858. (b) Horvat, Š.; MLinarić-Majerski, K.; Glavaš-Obrovac, L.; Jakas, A.; Veljković, J.; Marczi, S.; Kragol, G.; Roščić, M.; Matković, M.; Milostić-Srb, A. J. *Med. Chem.* **2006**, *49*, 3136−3142.

(5) Christensen, H. N.; Handlogten, M. E.; Lam, I.; Tager, H. S.; Zand, R. *J. Biol. Chem.* **1969**, *244*, 1510−1520.

(6) (a) Myers, R. M.; Shearman, J. W.; Kitching, M. O.; Ramos-Montoya, A.; Neal, D. E.; Ley, S. V. *ACS Chem. Biol.* **2009**, *4*, 503−525.

(7) Maffrand, J.-P.; Gully, D.; Boigegrain, R.; Jeanjean, F. *Actual. Chim. Thér.* **1994**, *21*, 171−179. The structure of SR 45398 reported by Sanofi in 1994 and 1995 was drawn with the appended N-linked phenyl group; in 1996 it was shown with the naphthyl group as shown in Figure 2. As there are no experimental details available, the true structure of this molecule cannot be definitively established.

(8) Boigegrain, R.; Gully, D.; Jeanjean, F.; Molimard, J. C. Eur. Pat. 0477049A1 1991 and Eur. Pat. 0477049B1, 1991.

(9) (a) Gully, D.; Labeeuw, B.; Boigegrain, R.; Oury-Donat, F.; Bachy, A.; Poncelet, M.; Steinberg, R.; Suaud-Chagny, M. F.; Santucci, V.; Vita, N.; Peccu, F.; Labbé-Jullié, C.; Kitagbi, P.; Soubrié, P.; Le Fur, G.; Maffrand, J.-P. *J. Pharmacol. Exp. Ther.* **1996**, *280*, 802−812. (b) Betancur, C.; Canton, M.; Burgos, A.; Labeeuw, B.; Gully, D.; Rosténe, W.; Pelaprat, D. *Eur. J. Pharmacol.* **1998**, *343*, 67−77.

(10) (a) Labbé-Jullié, C.; Barroso, S.; Nicolas-Etéve, D.; Reversat, J. L.; Botto, J. M.; Mazella, J.; Bernassau, J. M.; Kitabgi, P. *J. Biol. Chem.* **1998**, *273*, 16351−16357. (b) Kitabgi, P. *Peptides* **2006**, *27*, 2461−2468.

(11) (a) Nagasawa, H. T.; Elberling, J. A.; Shirota, F. N. *J. Med. Chem.* **1973**, *16*, 823−826. (b) Nagasawa, H. T.; Elberling, J. A.; Shirota, F. N. *J. Med. Chem.* **1975**, *18*, 826−830.

(12) (a) Baxendale, I. R.; Hayward, J. J.; Ley, S. V. *Comb. Chem. High Throughput Screening* **2007**, *10*, 802−836. (b) Glasnov, T. N.; Kappe, C. O. *Macromol. Rapid Commun.* **2007**, *28*, 395−410. (c) Glasnov, T. N.; Kappe, C. O. *Chem.—Eur. J.* **2011**, *17*, 11956−11968.

(13) (a) Arvela, R. K.; Leadbeater, N. E.; Collins, M. J., Jr. *Tetrahedron* **2005**, *61*, 9349−9355. (b) Pitts, M. R.; Baxendale, I. R. *Chim Oggi* **2006**, *24*, 41−45. (c) Moseley, J. D.; Woodman, E. K. *Org. Process Res. Dev.* **2008**, *12*, 967−981.

(14) Alternative commercial supplies of the 2-adamantanone, sodium cyanide, ammonium carbonate, and sodium hydroxide were obtained and tested, but no detectable difference in the composition of the product was obtained.

(15) (a) Pascal, R.; Tallades, J.; Commeyras, A. *Bull. Soc. Chim. Fr.* **1978**, *II*, 177−184. (b) Pascal, R.; Tallades, J.; Commeyras, A. *Tetrahedron* **1978**, *34*, 2275−2281. (c) Pascal, R.; Tallades, J.; Commeyras, A. *Tetrahedron* **1980**, *36*, 2999−3008. (d) Paventi, M.; Chubb, F. R.; Edward, J. T. *Can. J. Chem.* **1987**, *65*, 2114−2117.

(16) For some recent examples see: (a) Muñoz, M.; Alcázar, J.; de la Hoz, A.; Díaz-Ortiz, A. *Eur. J. Org. Chem.* **2012**, 260−263. (b) Seyler, H.; Jones, D. J.; Holmes, A. B.; Wong, W. H. H. *Chem. Commun.* **2012**, *48*, 1598−1600. (c) Ahmed-Omer, B.; Barrow, D. A.; Wirth, T.

ARKIVOC **2011**, *iv*, 26−36. (d) Rasheed, M.; Wirth, T. *Angew. Chem., Int. Ed.* **2011**, *50*, 357−358. (e) Martin, L. J.; Marzinzik, A. L.; Ley, S. V.; Baxendale, I. R. *Org. Lett.* **2011**, *13*, 320−323. (f) Rasheed, M.; Elmore, S. C.; Wirth, T. In *Catalytic Methods in Asymmetric Synthesis*; Gruttadauria, M., Giacalone, F., Eds.; John Wiley & Sons: New York, 2011, 345−371. (g) Ahmed-Omer, B.; Sanderson, A. J. *Org. Biomol. Chem.* **2011**, *9*, 3854−3862. (h) Smith, C. J.; Smith, C. D.; Nikbin, N.; Ley, S. V.; Baxendale, I. R. *Org. Biomol. Chem.* **2011**, *9*, 1927−1937. (i) Batoul, A.-O.; Sanderson, A. J. *Org. Biomol. Chem.* **2011**, *9*, 3854−3862. (j) Polyzos, A.; Baxendale, I. R.; Petersen, T.; Ley, S. V. *Angew. Chem., Int. Ed.* **2011**, *50*, 1190−1193. (k) Riva, E.; Rencurosi, A.; Gagliardi, S.; Passarella, D.; Martinelli, M. *Chem.—Eur. J.* **2011**, *17*, 6221−6226. (l) Lange, P. P.; Gooßen, L. J.; Podmore, P.; Underwood, T.; Sciammetta, N. *Chem. Commun.* **2011**, *47*, 3628−3630. (m) Brocklehurst, C. E.; Lehmann, H.; Vecchia, L. L. *Org. Process Res. Dev.* **2011**, *15*, 1447−1453. (n) Browne, D. L.; Deadman, B. J.; Ashe, R.; Baxendale, I. R.; Ley, S. V. *Org. Process Res. Dev* **2011**, *15*, 693−697. (o) Mercadante, M. A.; Leadbeater, N. E. *Org. Biomol. Chem.* **2011**, *9*, 6575−6578. (p) Bou-Hamdan, F. R.; Lévesque, F.; O'Brien, A. G.; Seeberger, P. H. *Beilstein J. Org. Chem.* **2011**, *7*, 1124−1129. (q) Wheeler, R. C.; Baxter, E.; Campbell, I. B.; Macdonald, S. J. F. *Org. Process Res. Dev.* **2011**, *15*, 565−569. (r) Qian, Z.; Baxendale, I. R.; Ley, S. V. *Synlett* **2010**, 505−508. (s) Malet-Sanz, L.; Madrzak, J.; S.V. Ley, S. V.; Baxendale, I. R. *Org. Biomol. Chem.* **2010**, *8*, 5324−5332. (t) Brasholz, M.; Macdonald, J. M.; Saubern, S.; Ryan, J. H.; Holmes, A. B. *Chem.—Eur. J.* **2010**, *16*, 11471−11480. (v) Wegner, J.; Ceylan, S.; Friese, C.; Kirschning, A. *Eur. J. Org. Chem.* **2010**, *23*, 4372. (w) Grafton, M.; Mansfield, A. C.; Fray, M. J. *Tetrahedron Lett.* **2010**, *51*, 1026−1029. (x) Tamborini, L.; Conti, P.; Pinto, A.; Micheli, C. D. *Tetrahedron: Asymmetry* **2010**, *21*, 222−225. (y) Hopkin, M. D.; Baxendale, I. R.; Ley, S. V. *Chem. Commun.* **2010**, *46*, 2450−2452.

(17) (a) Erlenmeyer, E. *Liebigs Ann. Chem* **1893**, *275*, 1−8. (b) Bergmann, M.; Stern, F.; Witte, C.; Liebigs. *Ann. Chem* **1926**, *449*, 277−302. (c) Crawford, M.; Little, W. T. *J. Chem. Soc.* **1959**, 729−731. (d) Steglich, W. *Fortschr. Chem. Forsch.* **1969**, *12*, 77−118. (e) Cornforth, J.; Ming-hui, D. *J. Chem. Soc., Perkin Trans. 1* **1991**, 2183−2187. (f) Combs, A. P.; Armstrong, R. W. *Tetrahedron Lett.* **1992**, *33*, 6419−6422. (g) Rasmussen, J. K.; Gleason, R. M.; Milbrath, D. S.; Rasmussen, R. L. *Ind. Eng. Chem. Res.* **2005**, *44*, 8554−8559.

(18) Greene, T.; Wuts, P. Protection of acetylenes. In *Protective Groups in Organic Synthesis*; Wiley-Interscience: New York, 1998.

(19) Browne, D. L.; Baumann, M.; Harji, B. H.; Baxendale, I. R.; Ley, S. V. *Org. Lett.* **2011**, *13*, 3312−3315.

(20) (a) It should be noted that liberation of acetylene does not occur upon the compound's melting at temperatures of 101.7 °C; the melting process is reproducible as such. (b) Due to the plastic crystalline nature of 2-adamantanone, two main peaks were detected when DSC scan was performed on the purchased material. Bazyleva, A. B.; Blokhin, A. V.; Kabo, G. J.; Kabo, A. G.; Sevruk, V. M. *Thermochim. Acta* **2006**, 65−72.

(21) (a) Sedelmeier, J.; Ley, S. V.; Baxendale, I. R.; Baumann, M. *Org. Lett.* **2010**, *12*, 3618−3621. (b) Battilocchio, C.; Baumann, M.; Baxendale, I. R.; Biava, M.; Kitching, M. O.; Ley, S. V.; Martin, R. E.; Ohnmacht, S. A.; Tappin, N. D. C. *Synthesis* **2012**, *44*, 635−647.

(22) (a) Brandt, J. C.; Elmore, S. C.; Robinson, R. I.; Wirth, T. *Synlett* **2010**, 3099−3103. (b) Audiger, L.; Watts, K.; Elmore, S. C.; Robinson, R. I.; Wirth, T. *ChemSusChem* **2011**, *5*, 257−260.

(23) Baumann, M.; Baxendale, I. R.; Martin, L. J.; Ley, S. V. *Tetrahedron* **2009**, *65*, 6611−6625.

(24) (a) Kovalskaya, S. S.; Dikusar, E. A.; Kozlov, N. G.; Popova, L. A. *Russ. J. Org. Chem.* **2001**, *37*, 1225−1227. (b) Schmidt, E. Y.; Vasil'tsov, A. M.; Mikhaleva, A. I.; Zaitsev, A. B.; Afonin, A. V.; Toryashinova, D. S. D.; Klyba, L. V.; Arndt, J. D.; Henkelmann, J. *ARKIVOC* **2003**, *xiii*, 35−44. (c) Hashmi, A. S. K.; Weyrauch, J. P.; Frey, W.; Bats, J. W. *Org. Lett.* **2004**, *6*, 4391−4394. (d) Jin, C.; Burgess, J. P.; Kepler, J. A.; Cook, C. E. *Org. Lett.* **2007**, *9*, 1887−1890. (e) Harmata, M.; Huang, C. *Synlett* **2008**, 1399−1401.

(25) Van Ornum, S. G.; Champeau, R. M.; Pariza, R. *Chem. Rev.* **2006**, *106*, 2990−3001.

(26) (a) Wada, Y.; Schmidt, M. A.; Jensen, K. F. *Ind. Eng. Chem. Res.* **2006**, *45*, 8036−8042. (b) Pelletier, M. J.; Fabiilli, M. L.; Moon, B. *Appl. Spectrosc.* **2007**, *61*, 1107−1115. (c) Hübner, S.; Bentrup, U.; Budde, U.; Lovis, K.; Dietrich, T.; Freitag, A.; Küpper, L.; Jähnisch, K. *Org. Process Res. Dev* **2009**, *13*, 952−960. (d) Carter, C. F.; Lange, H.; Baxendale, I. R.; Ley, S. V.; Goode, J.; Gaunt, N.; Wittkamp, B. *Org. Process Res. Dev.* **2010**, *14*, 393−404. (e) O'Brien, M.; Ian R. Baxendale, I. R.; Ley, S. V. *Org. Lett.* **2010**, *12*, 1596−1598. (f) Roydhouse, M. D.; Ghaini, A.; Constantinou, A.; Cantu-Perez, A.; Motherwell, W. B.; Gavriilidis, A. *Org. Process Res. Dev.* **2011**, *15*, 989−996.

(27) Ley, S. V.; Baxendale, I. R.; Bream, R. N.; Jackson, P. S.; Leach, A. G.; Longbottom, D. A.; Nessi, M.; Scott, J. S.; Storer, R. I.; Taylor, S. J. *J. Chem. Soc., Perkin Trans. 1* **2000**, 3815−4195.

(28) Gupta, D.; Soman, R.; Sukh, D. *Tetrahedron* **1982**, *38*, 3013−3018.

(29) (a) Jia, W.; Qiu, H.-H. *Exp. Thermal Fluid Sci.* **2003**, *27*, 829−838. (b) Horacek, B.; Kim, J.; Kiger, K. *IEEE Trans. Device Mater. Reliability* **2004**, *4*, 614−625. (c) Fisenko, S. P.; Wang, W.-N.; Lenggoro, I. W.; Okyuama, K. *Chem. Eng. Sci.* **2006**, *61*, 6029−6034.

(30) (a) Pantano, M.; Formaggio, F.; Crisma, M.; Bonora, G. M.; Mammi, S.; Peggion, E.; Toniolo, C.; Boesten, W. H. J.; Broxterman, Q. B.; Schoemaker, H. E.; Kamphius., J. *Macromolecules* **1993**, *26*, 1980−1984. (b) Antonova, A.; Simov., D. *Khimiya Geterotsikl. Soedin.* **1979**, *12*, 1587−1597.